

**Mesoscopic description of random walks on combs**Vicenç Méndez,<sup>1</sup> Alexander Iomin,<sup>2</sup> Daniel Campos,<sup>1</sup> and Werner Horsthemke<sup>3</sup><sup>1</sup>*Grup de Física Estadística, Departament de Física, Facultat de Ciències, Edifici Cc, Universitat Autònoma de Barcelona, 08193 Bellaterra (Barcelona), Spain*<sup>2</sup>*Department of Physics, Technion, Haifa 32000, Israel*<sup>3</sup>*Department of Chemistry, Southern Methodist University, Dallas, Texas 75275-0314, USA*

(Received 9 September 2015; revised manuscript received 29 October 2015; published 7 December 2015)

Combs are a simple caricature of various types of natural branched structures, which belong to the category of loopless graphs and consist of a backbone and branches. We study continuous time random walks on combs and present a generic method to obtain their transport properties. The random walk along the branches may be biased, and we account for the effect of the branches by renormalizing the waiting time probability distribution function for the motion along the backbone. We analyze the overall diffusion properties along the backbone and find normal diffusion, anomalous diffusion, and stochastic localization (diffusion failure), respectively, depending on the characteristics of the continuous time random walk along the branches, and compare our analytical results with stochastic simulations.

DOI: [10.1103/PhysRevE.92.062112](https://doi.org/10.1103/PhysRevE.92.062112)

PACS number(s): 05.40.–a

**I. INTRODUCTION**

Random walks often provide the underlying mesoscopic mechanism for transport phenomena in physics, chemistry, and biology [1–3]. A wide class of random walks gives rise to normal diffusion, where the mean-square displacement (MSD),  $\langle(\Delta r)^2(t)\rangle$ , grows linearly with time  $t$  for large times. In many important applications, however, the MSD behaves like  $\langle(\Delta r)^2(t)\rangle \propto t^\gamma$ , with  $\gamma \neq 1$ , and the diffusion is anomalous [1,2]. Anomalous diffusion can be modeled by various classes of random walks [4]. We focus on the important class of continuous time random walks (CTRWs) [1,2]. A specific feature of a CTRW is that a walker waits for a random time  $\tau$  between any two successive jumps. These waiting times are random independent variables with a probability distribution function (PDF)  $\phi(\tau)$ , and the tail of the PDF determines if the transport is diffusive ( $\gamma = 1$ ) or subdiffusive ( $\gamma < 1$ ). Heavy-tailed waiting time PDFs give rise to subdiffusion. Realistic models of the waiting time PDF have been formulated for transport in disordered materials with fractal and ramified architecture, such as porous discrete media [5] and comb and dendritic polymers [6–8], and for transport in crowded environments [9].

A simple caricature of various types of natural branched structures that belong to the category of loopless graphs is a comb model (see Fig. 1). The comb model was introduced to understand anomalous transport in percolation clusters [10–12]. Now, comblike models are widely employed to describe various experimental applications. These models have proven useful to describe the transport along spiny dendrites [13,14], percolation clusters with dangling bonds [11], diffusion of drugs in the circulatory system [15], energy transfer in comb polymers [6,7] and dendritic polymers [8], diffusion in porous materials [16–18], the influence of vegetation architecture on the diffusion of insects on plant surfaces [19], and many other interdisciplinary applications.

Simple random walks on comb structures provide a geometrical explanation of anomalous diffusion as happens also with walks on fractal structures. The excursion of the walker into the branches can be viewed as creating an effective waiting time

for the walk along the backbone [20], conferring a subdiffusive character on the transport; see, e.g., [11,21,22]. Several authors have determined various properties of walks on combs, such as the mean distance from the origin covered by a walker, the random walk dimension of the structure, the maximum deviation and span after a number of steps [22], and the spectral dimension and the mean first passage time for random walks on random and nontranslationally invariant combs [23] and for biased random walks [20]. Other studies have combined the complexity of combs with other statistical properties of the random walk. For example, a numerical study of the encounter problem of two walkers in branched structures shows that the topological heterogeneity of the structure can play an important role [24]. The hitting time between two arbitrary points of the comb and the mean first passage time in general  $d$ -dimensional combs has been determined in [25]. Further examples are the occupation time statistics for random walkers on combs where the branches can be regarded as independent complex structures, namely fractal or other ramified branches [26], and the effects of a magnetic field on a charged particle performing a random walk on a comb [27]. Finally, we want to mention studies to understand the diffusion mechanism along a variety of branched systems where scaling arguments, verified by numerical simulations, have been able to predict how the MSD grows with time [28].

Diffusion on comb structures has also been studied by macroscopic approaches, based on Fokker-Planck equations [12], which have been applied to describe diffusive properties in discrete systems, such as porous discrete media [5], infiltration of diffusing particles from one material into another [29], and superdiffusion due to the presence of inhomogeneous convection flow [30,31]. Other macroscopic descriptions, based on renormalizing the waiting time PDF for jumps along the backbone to take into account the transport along the branches [32], have been found useful to model continuous-time-reaction-transport processes [33] and human migrations along river networks [34].

Kahng and Redner provided a mesoscopic, probabilistic description of random walks on combs by using the successive decimation of the discrete-time master equation to obtain a

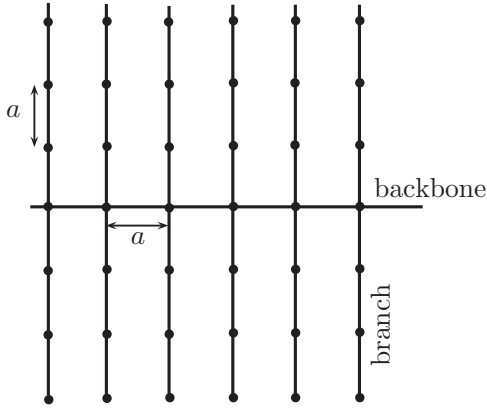


FIG. 1. Comb structure consisting of a backbone and branches. Each point represents a node where the walker may jump or wait a random time.

mesoscopic balance equation for the probability of the walker to be at a given node at a given time [35]. A mesoscopic approach is necessary for an accurate description of the transport properties, such as the diffusion coefficient or the mean visiting time in a branch, in terms of the parameters that characterize the random walk process.

Previous studies of random walks on combs have mostly considered Markovian walks, typically simple random walks where the particle makes one step on the structure at each discrete unit time interval. We consider the general case of non-Markovian random walks and adopt the formalism of CTRWs. We assume that the walker waits a random time distributed according to a general PDF  $\phi_0(\tau)$  at each node of the graph. The random waiting time may, for example, be due to binding-unbinding events at the nodes [9]. In addition, the walk along the branches may be biased. In the case of simple random walks, the excursions into the branches create a waiting time PDF for the motion along the backbone. This PDF depends on the interplay of the topology of the structure and the bias. In our case of non-Markovian random walks, the excursions into the branches modify the local waiting time PDF  $\phi_0(\tau)$ , a mesoscopic characteristic of the comb, and generate an effective waiting time PDF  $\phi(\tau)$  for the motion along the backbone of the comb. In other words, the non-Markovian CTRW on the comb can be reduced to a non-Markovian CTRW on a one-dimensional lattice, corresponding to the backbone only. We employ the decimation method of Kahng and Redner [35] to determine the effective waiting time PDF  $\phi(\tau)$ ; see also chapter 6.3 in [36]. The time spent by the walker between its entry into a branch and its return to the backbone for the first time is treated as a contribution to the effective waiting time at the node where the branch crosses the backbone. Our main results are exact analytic expressions for the effective waiting time PDF  $\phi(\tau)$  of the backbone motion and for key observables, such as the mean waiting time of the backbone dynamics, the diffusion coefficient, and the mean-square displacement, in terms of the mesoscopic characteristics of the walk, namely the local waiting PDF  $\phi_0(\tau)$ , the bias probability  $q$  along the branches, and the number of branch nodes  $N$ . We find that non-Markovian CTRWs on a comb can display three different

transport regimes: normal diffusion, anomalous diffusion, and stochastic localization.

The paper is organized as follows. In Sec. II, we formulate the mesoscopic description of the random walk on the comb and reduce the walker's motion to an effective motion along the backbone only with a renormalized waiting time PDF for the backbone nodes. Section III deals with the MSD of the effective backbone motion. The effective diffusion coefficient is derived, and the conditions for normal diffusion, anomalous diffusion, and stochastic localization (diffusion failure) [37] in terms of the number of branch nodes and the degree of bias of the motion along the branches are established. We summarize our results in Sec. IV.

## II. MESOSCOPIC DESCRIPTION

The simplest comb model, shown in Fig. 1, is formed by a principal axis, called the backbone, which is a one-dimensional lattice with spacing  $a$  and identical branches that cross the backbone perpendicularly at each node.

The walker moves through the comb by performing jumps between nearest-neighbor nodes along the backbone or along the branches. We assume that the walker performs isotropic jumps along the backbone, but the jumps along the branches may be biased, for example by an external field [10]. When the walker arrives at a node, it waits a random time  $\tau$  before performing a new jump to a nearest-neighbor node. We assume that the comb is homogeneous and the local waiting time PDF at any given node is given by  $\phi_0(\tau)$ .

When the walker enters a branch, it spends some time moving inside the branch before returning to the backbone. This sojourn time can be used to determine an effective waiting time PDF  $\phi(\tau)$  for the walker's motion along the backbone. In other words, the motion of the walker on the comb can be reduced to the effective motion along a one-dimensional lattice, corresponding to the backbone only. This motion is non-Markovian and can be described mesoscopically by the generalized master equation (GME) for the PDF  $P_{bb}(x, t)$  of finding the walker at node  $x$  on the backbone at time  $t$ :

$$\frac{\partial P_{bb}(x, t)}{\partial t} = \int_0^t K(t-t') dt' \left[ \int_{-\infty}^{\infty} P_{bb}(x-x', t') \Phi(x') dx' - P_{bb}(x, t') \right]. \quad (2.1)$$

Here,  $K(t)$  is the memory kernel related to the effective waiting time PDF via its Laplace transform,  $K(s) = s\phi(s)/[1-\phi(s)]$ , where  $s$  is the Laplace variable. The dispersal kernel  $\Phi(x)$  represents the probability of the walker performing a jump of length  $x$ . If the walker moves isotropically between nearest neighbors in a one-dimensional lattice of spacing  $a$ , the dispersal kernel reads  $\Phi(x) = \delta(x-a)/2 + \delta(x+a)/2$ . We assume that the walker is initially located at  $x=0$ , i.e.,  $P_{bb}(x, 0) = \delta_{x,0}$ , with  $x = ia$  and  $i = 0, \pm 1, \pm 2, \dots$ , where  $\delta_{x,0}$  is the Kronecker delta. Then the Laplace transform of the GME for  $x \neq 0$  reads

$$P_{bb}(x, s) = \frac{\phi(s)}{2} [P_{bb}(x-a, s) + P_{bb}(x+a, s)]. \quad (2.2)$$

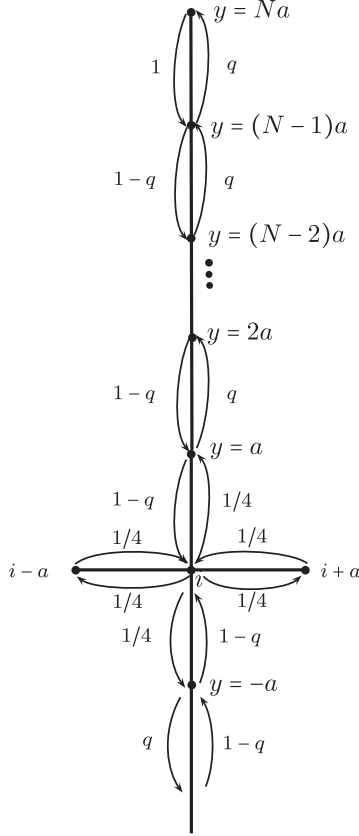


FIG. 2. Schematic representation of the possible jumps of a walker with the corresponding probabilities.

To derive the effective waiting time PDF  $\phi(t)$  for the backbone dynamics and relate it to the local waiting time PDF  $\phi_0(t)$  and the other mesoscopic characteristics of the comb, viz.  $q$  and  $N$ , we formulate the mesoscopic balance equation for the CTRW on the comb. Let  $P(x, y, t)$  be the PDF that the walker on the comb is located at the node with backbone coordinate  $x$  and branch coordinate  $y$  at time  $t$ , and let  $P(x, y, s)$  be its Laplace transform. Taking into account the contributions of the walker arriving from the upper and lower branch (see Fig. 2), we obtain the mesoscopic balance equation for the walker being at node  $(x, y) = (ia, 0)$ , i.e., being at a backbone node,

$$P(x, s) = \frac{\phi_0(s)}{4} [P(x - a, s) + P(x + a, s)] + (1 - q)\phi_0(s)[P(y = a, s) + P(y = -a, s)]. \quad (2.3)$$

To achieve a concise notation, we are using  $P(x, s)$ ,  $P(x - a, s)$ , and  $P(x + a, s)$  as shorthand for  $P(x, y = 0, s)$ ,  $P(x - a, y = 0, s)$ , and  $P(x + a, y = 0, s)$ , and  $P(y = a, s)$  and  $P(y = -a, s)$  stand for  $P(x, y = a, s)$  and  $P(x, y = -a, s)$ , respectively.

The term  $\phi_0(s)[P(x - a, s) + P(x + a, s)]/4$  corresponds to the contribution of the walker arriving at node  $x = ia$  from the left or from the right with probability  $1/4$  after waiting a random time  $\tau$  with PDF  $\phi_0(\tau)$  at nodes  $x + a$  or  $x - a$ .

As shown in Fig. 2, the walker located at the  $i$ th node of the backbone may jump to the right, left, up, or down with

probability  $1/4$ . We assume that the walker moves forward (away from the backbone) along the branches with probability  $q$  and back to the backbone with probability  $1 - q$ . The term

$$(1 - q)\phi_0(s)[P(y = a, s) + P(y = -a, s)] \quad (2.4)$$

in (2.3) corresponds the contribution of the walker arriving at the backbone node  $x$  from the first node of the upper or lower branch after waiting there a random time  $\tau$  with PDF  $\phi_0(\tau)$ .

If we can express  $P(y = a, s)$  and  $P(y = -a, s)$  in (2.3) in terms of  $P(x, s)$ , then (2.3) can be cast in the form of (2.2). In other words, any contribution from branch nodes will have been eliminated and we will obtain a closed balance equation for  $P(x, s) = P(x, y = 0, s)$  purely in terms of the probabilities of the walker being at adjacent backbone nodes. We can then identify  $P(x, s)$  with  $P_{bb}(x, s)$  and replace the CTRW on the comb by an effective CTRW on a one-dimensional lattice, corresponding to the backbone. This effective walk accounts for the excursions of the walker on the comb into the side branches in terms of an effective waiting time PDF  $\phi(\tau)$  at backbone nodes.

We proceed as follows. Consider the motion along the upper branches. The lower branch dynamics is the same due to the symmetry of the comb. The mesoscopic balance equation for the first node of the upper branches reads

$$P(y = a, s) = \frac{\phi_0(s)}{4} P(x, s) + \phi_0(s)(1 - q)P(y = 2a, s). \quad (2.5)$$

The first term  $\phi_0(s)P(x, s)/4$  corresponds to the contribution of the walker arriving from the backbone, while  $\phi_0(s)(1 - q)P(y = 2a, s)$  is the contribution of the walker jumping from the upper node  $y = 2a$  to  $y = a$  with probability  $1 - q$  after waiting a random time  $\tau$  with PDF  $\phi_0(\tau)$ . Analogously, we have, for the lower branches,

$$P(y = -a, s) = \frac{\phi_0(s)}{4} P(x, s) + \phi_0(s)(1 - q)P(y = -2a, s). \quad (2.6)$$

We now need to relate  $P(y = \pm 2a, s)$  to  $P(y = \pm a, s)$  to close (2.5) and (2.6). After some calculations (see the Appendix for details), we find

$$P(y = \pm 2a, s) = G(q, \phi_0(s))P(y = \pm a, s), \quad (2.7)$$

where

$$G(q, \phi_0(s)) = \frac{2q\phi_0(s)}{1 + \frac{1 + H(q, \phi_0(s))}{1 - H(q, \phi_0(s))} \sqrt{1 - 4q(1 - q)\phi_0^2(s)}}, \quad (2.8)$$

$$H(q, \phi_0(s)) = \left( \frac{\lambda_-}{\lambda_+} \right)^{N-5} \frac{\lambda_- - h(\phi_0(s))}{\lambda_+ - h(\phi_0(s))}, \quad (2.9)$$

and

$$h(\phi_0(s)) = \frac{q\phi_0(s)[1 - q\phi_0^2(s)]}{1 + q(q - 2)\phi_0^2(s)}. \quad (2.10)$$

Substituting (2.7) into (2.5) and (2.6) and using the resulting expressions in (2.3), we obtain an equation of the form (2.2)

with

$$\phi(s) = \frac{\phi_0(s)}{2 - \frac{(1-q)\phi_0^2(s)}{1 - (1-q)\phi_0(s)G(q, \phi_0(s))}}, \quad (2.11)$$

whose Laplace inversion yields  $\phi(\tau)$ . The waiting time PDF  $\phi(\tau)$  incorporates the dynamics along the branches and can be understood as the effective waiting time PDF for a walker moving along the backbone only. This is our first main result. We have derived an exact analytical expression for the effective waiting time PDF  $\phi(\tau)$  of the backbone dynamics in terms of the mesoscopic characteristics of the random walk on the comb, namely the local waiting time PDF  $\phi_0(\tau)$ , the bias probability  $q$ , and the number of branch nodes  $N$ . This result allows us to obtain exact analytical expressions for key observables of the transport on the comb, as we show in the next section.

### III. STATISTICAL PROPERTIES

#### A. $N$ finite

If the local waiting time PDF  $\phi_0(\tau)$  has finite moments, its Laplace transform reads [2]  $\phi_0(s) \simeq 1 - s\bar{t}$  in the large time limit  $s \rightarrow 0$ , where  $\bar{t}$  is the local mean waiting time at each node. Taking the limit  $s \rightarrow 0$  in (2.11), we obtain the effective waiting time PDF for the backbone dynamics,

$$\phi(s) \simeq (1 + s\langle t \rangle)^{-1}. \quad (3.1)$$

The effective mean waiting time  $\langle t \rangle$  for backbone nodes is given by

$$\langle t \rangle = \frac{\bar{t}}{2q-1} [2(1-q)^{1-N}q^N + 4q - 3]. \quad (3.2)$$

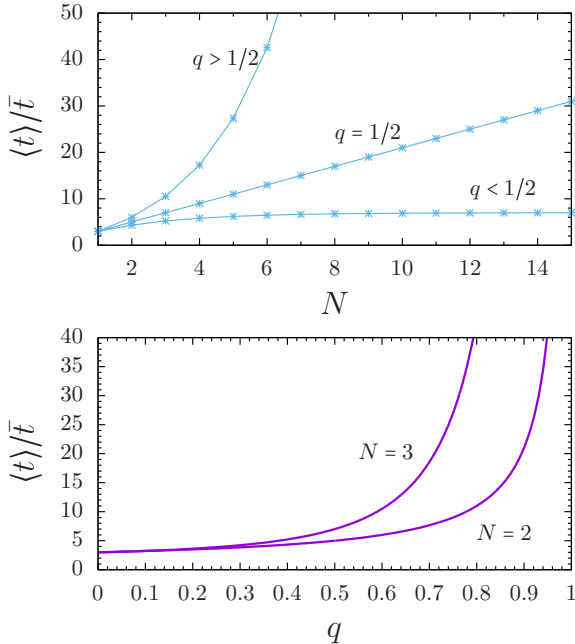


FIG. 3. (Color online) Dimensionless mean waiting time of the effective backbone dynamics.

In Fig. 3, we plot this effective mean waiting time versus  $N$  and  $q$ . The mean waiting time  $\langle t \rangle$  is a monotonically increasing function of both  $q$  and  $N$ . If the random walk inside the branches is isotropic,  $q = 1/2$ , we obtain by l'Hôpital's rule from (3.2),

$$\lim_{q \rightarrow 1/2} \langle t \rangle = (1 + 2N)\bar{t}. \quad (3.3)$$

To determine the diffusion coefficient  $D$  for diffusion through the comb, we first calculate the MSD. Performing the Fourier-Laplace transform on (2.1), we obtain

$$P(k, s) = \frac{1 - \phi(s)}{s[1 - \Phi(k)\phi(s)]}. \quad (3.4)$$

The MSD in Laplace space reads (see, e.g., [2])

$$\langle x^2(s) \rangle = - \lim_{k \rightarrow 0} \frac{d^2 P(k, s)}{dk^2}. \quad (3.5)$$

As mentioned in Sec. II, we assume that the motion on the backbone is unbiased and that the walker only jumps to nearest neighbors. This implies that the kernel  $\Phi(x)$  is given by  $\Phi(x) = \delta(x - a)/2 + \delta(x + a)/2$ , and we obtain, from (3.5),

$$\langle x^2(s) \rangle = \frac{a^2}{s[\phi(s)^{-1} - 1]}. \quad (3.6)$$

If the local waiting time PDF  $\phi_0(t)$  possesses a finite first moment, then so does the effective waiting time PDF  $\phi(t)$  [see (3.1)], and the MSD along the backbone corresponds to normal diffusion,  $\langle x^2(t) \rangle = 2Dt$ . The diffusion coefficient is given by

$$D = \frac{a^2}{2\langle t \rangle} = \frac{a^2}{2\bar{t}} \frac{2q - 1}{2(1-q)^{1-N}q^N + 4q - 3}. \quad (3.7)$$

Note that in the limit of an isotropic random walk ( $q = 1/2$ ),  $D$  behaves like  $N^{-1}$  for large  $N$  by virtue of (3.3) and (3.7), in agreement with the scaling results found in [38]. In Fig. 4, we compare the result provided by (3.7) with numerical simulations. As Fig. 3 demonstrates,  $\langle t \rangle$  increases monotonically with  $N$  for  $q < 1/2$  and saturates at  $(4q - 3)/(2q - 1)$  for  $N \rightarrow \infty$ . Consequently, the mean waiting time  $\langle t \rangle$  is finite for

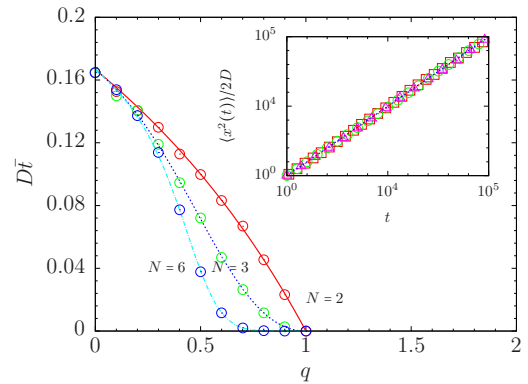


FIG. 4. (Color online) Plot of the diffusion coefficient for transport through the comb for  $N = 2$ ,  $N = 3$ , and  $N = 6$  vs  $q$  with  $a = 1$ . Solid curves correspond to exact analytical results given by (3.7). Results from numerical simulations are depicted with symbols. Inset: MSD/ $2D$  for  $N = 5$  and three different values of  $q$ :  $q = 0.4$  (squares),  $q = 0.5$  (circles), and  $q = 0.6$  (triangles).

$N \rightarrow \infty$ ; the overall diffusion along the backbone is normal. However, for  $q \geq 1/2$ , the mean waiting time  $\langle t \rangle$  increases without bound as  $N$  increases, and anomalous transport is expected for  $N \rightarrow \infty$ . In Fig. 4 (inset), we plot the MSD scaled by the diffusion coefficient. It illustrates the result given by (3.7) for the MSD. The transport is diffusive for finite  $N$ , regardless of the value of  $q$  and the specific form of the local waiting time PDF  $\phi_0(\tau)$ , as long as the latter has finite moments.

We consider now the case of a local waiting time PDF with the large time limit  $\phi_0(\tau) \sim \tau^{-1-\gamma}$ , with Laplace transform  $\phi_0(s) \simeq 1 - (s\tau_0)^\gamma$  and  $0 < \gamma < 1$ , which does not possess finite moments. Here  $\tau_0$  is a parameter with units of time. In this case, the effective waiting time PDF for the backbone dynamics is obtained by simply replacing  $s\bar{t}$  with  $(s\tau_0)^\gamma$ , and (3.1) reads  $\phi(s) \simeq [1 + (s\tau_0)^\gamma \langle t \rangle / \tau_0]^{-1}$ . Substituting this result into (3.6), we find

$$\langle x^2(t) \rangle = \frac{a^2 \tau_0}{\langle t \rangle} \frac{(t/\tau_0)^\gamma}{\Gamma(1 + \gamma)}, \quad (3.8)$$

for large  $t$ , where  $\langle t \rangle$  is given by (3.2), with  $\tau_0$  instead of  $\bar{t}$ . If the local waiting time PDF  $\phi_0(\tau)$  at each node of the comb has a power-law tail, then the overall transport along the backbone is anomalous. Note that the anomaly exponent of the effective backbone transport is the same as the anomaly exponent of the CTRW on the comb.

### B. $N \rightarrow \infty$

If the number of nodes of the branches goes to infinity, the mean time spent by the walker visiting a branch increases monotonically; see (3.2). If the diffusion coefficient tends asymptotically to a constant, which is the case for  $q < 1/2$ , the diffusive scaling will saturate at  $D = a^2(2q - 1)/[2\bar{t}(4q - 3)]$ , according to (3.7). For  $q \geq 1/2$ , the limit  $N \rightarrow \infty$  leads to  $D \rightarrow 0$  and we expect a different scaling. For  $N \rightarrow \infty$ , the quotient  $(\lambda_-/\lambda_+)^N \rightarrow 0$  and also  $H \rightarrow 0$ . We obtain, from (2.8),

$$G(q, \phi_0(s)) = \frac{2q\phi_0(s)}{1 + \sqrt{1 - 4q(1 - q)\phi_0^2(s)}} \equiv \frac{2q\phi_0(s)}{1 + g(q)}, \quad (3.9)$$

where we define  $g(q) \equiv \sqrt{1 - 4q(1 - q)\phi_0^2(s)}$  for convenience. Equation (2.11) for the Laplace transform of the effective waiting time PDF reduces to

$$\phi(s) = \frac{\phi_0(s)[1 + g(q) - 2q(1 - q)\phi_0^2(s)]}{2 - (1 + 3q - 4q^2)\phi_0^2(s) + [2 - (1 - q)\phi_0^2(s)]g(q)}. \quad (3.10)$$

We take the limit  $s \rightarrow 0$  and consider first the case where the local waiting time PDF  $\phi_0(\tau)$  has finite moments. Then  $\phi_0(s) \simeq 1 - s\bar{t}$ , as  $s \rightarrow 0$ , and the effective waiting time PDF of the backbone dynamics is given by

$$\phi(s) \simeq \begin{cases} (1 + \frac{4q-3}{2q-1}s\bar{t})^{-1}, & q < 1/2 \\ (1 + \sqrt{2s\bar{t}})^{-1}, & q = 1/2 \\ [\frac{3q-1}{q} + \frac{4q^2-3q+1}{(2q-1)q}s\bar{t}]^{-1}, & q > 1/2. \end{cases} \quad (3.11)$$

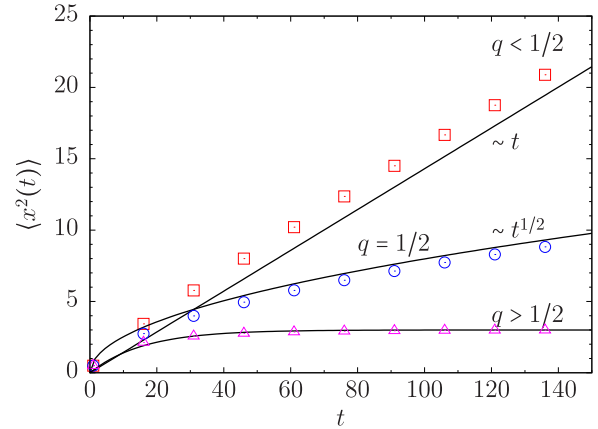


FIG. 5. (Color online) MSD for three values of  $q$ , displaying the three different transport regimes. Solid curves correspond to the results given by (3.12) for  $q = 0.4$ ,  $q = 0.5$ , and  $q = 0.6$ . Symbols correspond to the results of numerical simulations with  $N = 10^4$  and  $a = 1$ .

Substituting (3.11) into (3.6), we find, for large  $t$ ,

$$\langle x^2(t) \rangle = \begin{cases} a^2 \frac{2q-1}{4q-3} \frac{t}{\bar{t}}, & q < 1/2 \\ a^2 \sqrt{\frac{2t}{\pi\bar{t}}}, & q = 1/2 \\ a^2 \frac{q}{2q-1} (1 - e^{-\alpha t}), & q > 1/2, \end{cases} \quad (3.12)$$

where the rate of saturation is

$$\alpha = \frac{(2q - 1)^2}{(4q^2 - 3q + 1)\bar{t}}. \quad (3.13)$$

In Fig. 5, we compare these results with numerical simulations for  $N = 10^4$ . For  $q = 1/2$ , we obtain the well-known result of subdiffusive transport with the MSD  $\sim \sqrt{t}$ . However, for  $q \neq 1/2$ , the side branches experience advection and the transport is remarkably different. Namely, for  $q > 1/2$ , the advection is away from the backbone along the branches,  $y \rightarrow \pm\infty$ . The walker is effectively trapped inside the branches and stochastic localization (diffusion failure) occurs,  $\langle x^2(\infty) \rangle < \infty$  [37]. For  $q < 1/2$ , the advection is towards the backbone. It enhances the backbone dynamics and normal diffusion takes place.

Of course the limit  $N \rightarrow \infty$  cannot be attained in a strict sense for real systems. However, transport on a comb structure will display the behavior discussed above for sufficiently large  $N$ . Note that the numerical results in Fig. 5 were obtained for  $N = 10^4$ . On the other hand, we expect that (3.12) holds experimentally only up to a large finite time, namely as long as the walker does not experience the finite size of the branches. This is illustrated in Fig. 6, where we have used an intermediate value  $N = 100$ . We show only the case  $q = 1/2$  for easier visualization. We clearly observe that the result (3.12) holds for an intermediate time regime. For large times, when the walkers have had time to reach the extremes of the branches and return to the backbone, the diffusive scaling, with  $D$  given by (3.7), is recovered. This is in agreement with the scaling results for the dynamical crossover obtained in [38].

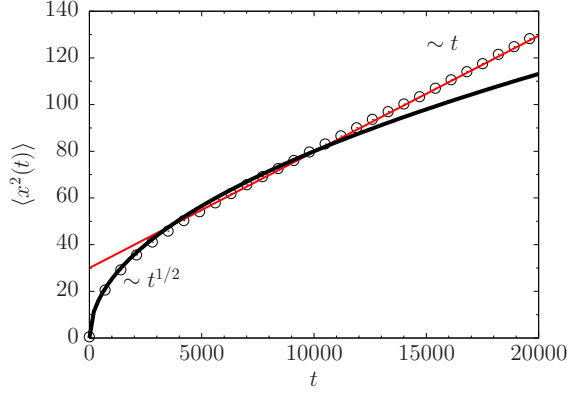


FIG. 6. (Color online) MSD behavior for  $q = 1/2$  for large  $N$ . Here,  $N = 100$  is used. The numerical results (circles) fit the result (3.12) for intermediate times, as if the branches were infinite. For large times, the linear scaling corresponding to finite  $N$  is recovered.

We consider now the case where the local waiting time PDF is  $\phi_0(\tau) \sim \tau^{-1-\gamma}$ , i.e.,  $\phi_0(s) \simeq 1 - (s\tau_0)^\gamma$  with  $0 < \gamma < 1$ , as  $s \rightarrow 0$ . The MSD in this case can be obtained straightforwardly by replacing  $s\bar{t}$  with  $(s\tau_0)^\gamma$  in (3.11). For large times, it reads

$$\langle x^2(t) \rangle = \begin{cases} \frac{a^2}{\Gamma(1+\gamma)} \frac{2q-1}{4q-3} \left(\frac{t}{\tau_0}\right)^\gamma, & q < 1/2 \\ \frac{a^2}{\sqrt{2}\Gamma(1+\gamma/2)} \left(\frac{t}{\tau_0}\right)^{\gamma/2}, & q = 1/2 \\ \frac{a^2 q(2q-1)}{(4q^2-3q+1)} \mu(t/\tau_0), & q > 1/2, \end{cases} \quad (3.14)$$

where

$$\mu(t/\tau_0) = (t/\tau_0)^\gamma E_{\gamma,\gamma+1} \left[ - \left(\frac{t}{\tau_0}\right)^\gamma \frac{(2q-1)^2}{4q^2-3q+1} \right] \quad (3.15)$$

is expressed in terms of the generalized Mittag-Leffler function  $E_{\alpha,\beta}(z)$ . We use the following property of integration of the Mittag-Leffler function [39]:

$$\int_0^t E_{\alpha,\beta}(bz^\alpha) z^{\beta-1} dz = t^\beta E_{\alpha,\beta+1}(bt^\alpha). \quad (3.16)$$

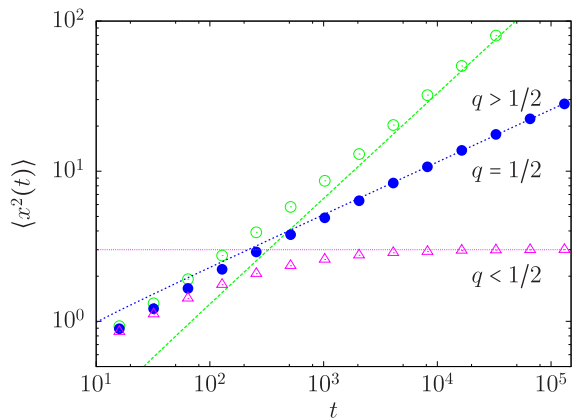


FIG. 7. (Color online) MSD for three values of  $q$ , displaying the different transport regimes, for  $\gamma = 0.7$ . Lines correspond to the asymptotic results given by (3.14) for  $q = 0.4$ ,  $q = 0.5$ , and  $q = 0.6$ . Symbols correspond to results from numerical simulations with  $N = 10^4$ ,  $a = 1$ , and  $t_{\min} = 1$ .

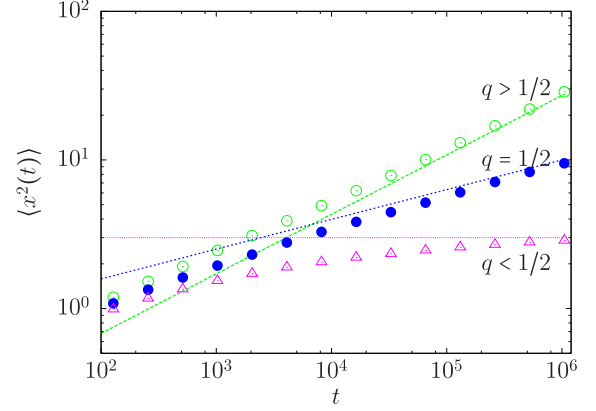


FIG. 8. (Color online) MSD for three values of  $q$ , displaying the different transport regimes, for  $\gamma = 0.4$ . Lines correspond to the asymptotic results given by (3.14) for  $q = 0.4$ ,  $q = 0.5$ , and  $q = 0.6$ . Symbols correspond to results from numerical simulations with  $N = 10^4$ ,  $a = 1$ , and  $t_{\min} = 1$ .

Subdiffusion in the branches results in backbone subdiffusion for  $q \leq 1/2$ . For advection towards the backbone,  $q < 1/2$ , the anomaly exponent of the effective backbone transport is the same as the anomaly exponent of the CTRW on the comb. For the case of no bias,  $q = 1/2$ , the anomaly exponent of the effective backbone transport is half that of the CTRW on the comb. For advection away from the backbone,  $q > 1/2$ , we again find stochastic localization. For  $t/\tau_0 \gg 1$ ,  $E_{\alpha,\beta}(-at^\alpha) \sim t^{-\alpha}/\Gamma(\beta - \alpha)$  [40], and, consequently,  $\mu(t/\tau_0)$  approaches a finite value as  $t \rightarrow \infty$ .

The validity of (3.14) is confirmed by the numerical results shown in Figs. 7 and 8, which are the analog of Fig. 5, for  $\gamma = 0.7$  and  $\gamma = 0.4$ , respectively. The numerical results were obtained by explicitly introducing waiting times between jumps in the random walk process along the comb structure. These random times were generated according to the PDF  $\phi_0(t) = \gamma t_{\min}^{-1} (t/t_{\min})^{-1-\gamma}$  defined for the interval  $t > t_{\min}$ . Note that this choice leads straightforwardly to the desired asymptotic behavior  $\phi_0(s) \simeq 1 - (s\tau_0)^\gamma$  in Laplace space, with  $\tau_0^\gamma = \gamma \pi \csc[(1+\gamma)\pi]/\Gamma(1+\gamma)$ .

#### IV. CONCLUSION

We have derived an effective mesoscopic equation, given by (2.2) and (2.11), for a random walk on a regular comb structure. The random walk along the branches consists of possibly biased jumps to the nearest-neighbor nodes, while the walker waits at each node for a random time  $\tau$  distributed according to the local waiting time PDF  $\phi_0(\tau)$  before proceeding with the next jump. The overall dynamics along the branches has been reduced to an effective waiting time PDF  $\phi(\tau)$ , given by (2.11), for motion solely along the backbone. We have obtained exact analytical expressions for the statistical properties, such as the effective mean waiting time  $\langle t \rangle$  for the backbone nodes, the diffusion coefficient  $D$ , and the MSD of the overall structure in terms of the bias probability  $q$  for the cases where the number of nodes  $N$  of the branches is finite or infinite. We have established that a comb can display normal diffusion,

subdiffusion, and stochastic localization, which is dependent on the characteristic parameters of the CTRW.

If  $N$  is finite and the local waiting time PDF  $\phi_0(\tau)$  has finite moments, exact expressions for both  $\langle t \rangle$  and  $D$  are derived analytically in terms of the bias probability  $q$ , the number of nodes  $N$  on the branch, and the mean waiting time probability at each node. The transport always corresponds to normal diffusion in this case. If the local waiting time PDF  $\phi_0(\tau) \sim \tau^{-1-\gamma}$  for large time, it does not possess finite moments and the MSD of the random walker along the backbone behaves like  $t^\gamma$ . The transport on the comb corresponds to anomalous diffusion.

If  $N$  is infinite, the value of  $q$  is the crucial factor. If the local waiting time PDF  $\phi_0(\tau)$  has finite moments, then the transport corresponds to normal diffusion for  $q < 1/2$ . If  $q = 1/2$ , the MSD behaves like  $t^{1/2}$ , and the transport is subdiffusive. If  $q > 1/2$ , the MSD approaches a constant finite value for large time, corresponding to stochastic localization (diffusion failure). If the local waiting time PDF  $\phi_0(\tau)$  does not have finite moments,  $\phi_0(\tau) \sim \tau^{-1-\gamma}$  for large time, then the MSD behaves like  $t^\gamma$  for  $q < 1/2$  and like  $t^{\gamma/2}$  for  $q = 1/2$ ; the transport is subdiffusive. Stochastic localization occurs again for  $q > 1/2$ . In all cases, the theoretical predictions have been verified by numerical simulations. In summary, if the bias probability of moving away from the backbone is  $q > 1/2$ , then stochastic localization occurs, regardless of the other characteristic parameters related to the random walk on the branches.

#### ACKNOWLEDGMENTS

A.I. would like to thank the Universitat Autònoma de Barcelona for hospitality and financial support, as well as the support by the Israel Science Foundation (Grant No. ISF-1028). V.M. and D.C. have been supported by the Ministerio de Economía y Competitividad under Grant No. FIS2012-32334 and by Generalitat de Catalunya under Grant No. SGR2014-923. V.M. also thanks the Isaac Newton Institute for Mathematical Sciences, Cambridge, for support and hospitality during the CGP programme, where part of this work was undertaken.

#### APPENDIX: DERIVATION OF EQ. (2.7)

Generalizing (2.5) to any node of the branches located between  $2a \leq y \leq (N-2)a$ , we obtain the balance equation for the upper branches,

$$P(y,s) = \phi_0(s)[qP(y-a,s) + (1-q)P(y+a,s)], \quad (\text{A1})$$

where  $P(y,t)$  is shorthand for  $P(x,y,t)$ , the PDF of finding the walker at time  $t$  at node  $y$  on the branch originating at  $x$  from the backbone, and  $P(y,s)$  is its Laplace transform.

To determine the Laplace transform  $\phi(s)$  of the effective backbone node waiting time PDF, we need to determine  $P(y = a,s)$  and  $P(y = -a,s)$  in (2.3) in terms of  $P(x,s)$ , so that (2.3) can be cast in the form of (2.2). Given (2.5) and (2.6), this goal can be achieved if  $P(y = 2a,s)$  and  $P(y = -2a,s)$  can be related to  $P(y = a,s)$  and  $P(y = -a,s)$ . We proceed as

follows. The solution of (A1) reads

$$P(y,s) = A_1 \lambda_+^{y/a} + A_2 \lambda_-^{y/a}, \quad (\text{A2})$$

where

$$\lambda_{\pm} = \frac{1 \pm \sqrt{1 - 4q(1-q)\phi_0^2(s)}}{2(1-q)\phi_0(s)}. \quad (\text{A3})$$

To find expressions for the quantities  $A_1$  and  $A_2$ , whose dependence on  $x$  and  $s$  is not displayed, we apply (A2) to the node  $y = 2a$ :

$$P(y = 2a,s) = A_1 \lambda_+^2 + A_2 \lambda_-^2. \quad (\text{A4})$$

On the other hand, setting  $y = 2a$  in (A1), we find

$$\begin{aligned} P(y = 2a,s) - \phi_0(s)qP(y = a,s) \\ = \phi_0(s)(1-q)P(y = 3a,s). \end{aligned} \quad (\text{A5})$$

Setting  $y = 3a$  in (A2), we obtain

$$\begin{aligned} P(y = 2a,s) - q\phi_0(s)P(y = a,s) \\ = \phi_0(s)(1-q)[A_1 \lambda_+^3 + A_2 \lambda_-^3]. \end{aligned} \quad (\text{A6})$$

Solving the system of Eqs. (A4) and (A6) for the quantities  $A_1$  and  $A_2$ , we obtain

$$A_1 = \frac{P(y = 2a,s) - q\phi_0(s)P(y = a,s)}{\lambda_+^2(\lambda_+ - \lambda_-)\phi_0(s)(1-q)} - \frac{\lambda_- P(y = 2a,s)}{\lambda_+^2(\lambda_+ - \lambda_-)}, \quad (\text{A7})$$

$$\begin{aligned} A_2 = \frac{-P(y = 2a,s) + q\phi_0(s)P(y = a,s)}{\lambda_-^2(\lambda_+ - \lambda_-)\phi_0(s)(1-q)} \\ + \frac{\lambda_+ P(y = 2a,s)}{\lambda_-^2(\lambda_+ - \lambda_-)}. \end{aligned} \quad (\text{A8})$$

A special situation occurs at the end of the branches, where we have to impose reflecting boundary conditions, i.e.,

$$P(y = Na,s) = q\phi_0(s)P[y = (N-1)a,s]. \quad (\text{A9})$$

The node at  $y = (N-1)a$  also needs a special balance equation (see Fig. 2),

$$\begin{aligned} P[y = (N-1)a,s] = q\phi_0(s)P[y = (N-2)a,s] \\ + \phi_0(s)P(y = Na,s). \end{aligned} \quad (\text{A10})$$

Substituting  $y = (N-2)a$  into (A1) and taking into account (A9), we can write

$$P[y = (N-2)a,s] = h(\phi_0(s))P[y = (N-3)a,s], \quad (\text{A11})$$

where

$$h(\phi_0(s)) = \frac{q\phi_0(s)[1 - q\phi_0^2(s)]}{1 + q(q-2)\phi_0^2(s)}. \quad (\text{A12})$$

Substituting the solutions from (A2), (A7), and (A8) into (A11), we find

$$P(y = 2a,s) = G(q,\phi_0(s))P(y = a,s), \quad (\text{A13})$$

where

$$G(q, \phi_0(s)) = \frac{2q\phi_0(s)}{1 + \frac{1 + H(q, \phi_0(s))}{1 - H(q, \phi_0(s))} \sqrt{1 - 4q(1 - q)\phi_0^2(s)}}, \quad (\text{A14})$$

$$H(q, \phi_0(s)) = \left( \frac{\lambda_-}{\lambda_+} \right)^{N-5} \frac{\lambda_- - h(\phi_0(s))}{\lambda_+ - h(\phi_0(s))}. \quad (\text{A15})$$

For the lower branch, we obtain, in a similar manner,

$$P(y = -2a, s) = G(q, \phi_0(s))P(y = -a, s). \quad (\text{A16})$$

We have achieved our goal of expressing  $P(y = 2a, s)$  and  $P(y = -2a, s)$  in terms of  $P(y = a, s)$  and  $P(y = -a, s)$ .

- 
- [1] E. W. Montroll and M. F. Shlesinger, On the wonderful world of random walks, in *Nonequilibrium Phenomena II: From Stochastics to Hydrodynamics*, edited by J. L. Lebowitz and E. W. Montroll (Elsevier Science, Amsterdam, 1984), p. 1.
- [2] R. Metzler and J. Klafter, The random walk's guide to anomalous diffusion: A fractional dynamics approach, *Phys. Rep.* **339**, 1 (2000).
- [3] J. Klafter and I. M. Sokolov, *First Steps in Random Walks: From Tools to Applications* (Oxford University Press, New York, 2011).
- [4] R. Metzler and J. Klafter, The restaurant at the end of the random walk: recent developments in the description of anomalous transport by fractional dynamics, *J. Phys. A: Math. Gen.* **37**, R161 (2004).
- [5] K. Maex, M. R. Baklanov, D. Shamiryana, F. Iacopi, S. H. Brongersma, and Z. S. Yanovitskaya, Low dielectric constant materials for microelectronics, *J. Appl. Phys.* **93**, 8793 (2003).
- [6] E. F. Casassa and G. C. Berry, Angular distribution of intensity of Rayleigh scattering from comblike branched molecules, *J. Polymer Sci. A* **4**, 881 (1966).
- [7] J. F. Douglas, J. Roovers, and K. F. Freed, Characterization of branching architecture through universal ratios of polymer solution properties, *Macromolecules* **23**, 4168 (1990).
- [8] H. Frauenrath, Dendronized polymers—building a new bridge from molecules to nanoscopic objects, *Prog. Polymer Sci.* **30**, 325 (2005).
- [9] I. M. Sokolov, Models of anomalous diffusion in crowded environments, *Soft Matter* **8**, 9043 (2012).
- [10] S. R. White and M. Barma, Field-induced drift and trapping in percolation networks, *J. Phys. A: Math. Gen.* **17**, 2995 (1984).
- [11] G. H. Weiss and S. Havlin, Some properties of a random walk on a comb structure, *Physica A* **134**, 474 (1986).
- [12] V. E. Arkhincheev and E. M. Baskin, Anomalous diffusion and drift in a comb model of percolation clusters, *Zh. Eksp. Teor. Fiz.* **100**, 292 (1991) [*Sov. Phys. JETP* **73**, 161 (1991)].
- [13] V. Méndez and A. Iomin, Comb-like models for transport along spiny dendrites, *Chaos Solitons Fractals* **53**, 46 (2013).
- [14] A. Iomin and V. Méndez, Reaction-subdiffusion front propagation in a comblike model of spiny dendrites, *Phys. Rev. E* **88**, 012706 (2013).
- [15] R. E. Marsh, T. A. Riauka, and S. A. McQuarrie, A review of basic principles of fractals and their application to pharmacokinetics, *Q. J. Nucl. Med. Mol. Imaging* **52**, 278 (2008).
- [16] V. E. Arkhincheev, E. Kunnen, and M. R. Baklanov, Active species in porous media: Random walk and capture in traps, *Microelectron. Eng.* **88**, 694 (2011).
- [17] H. E. Stanley and A. Coniglio, Flow in porous media: The backbone fractal at the percolation threshold, *Phys. Rev. B* **29**, 522 (1984).
- [18] A. Tarasenko and L. Jastrabík, A one-dimensional lattice-gas model for simulating diffusion in channel pores with side pockets: The analytical approach and kinetic Monte Carlo technique, *Microporous Mesoporous Mater.* **152**, 134 (2012).
- [19] S. Hannunen, Vegetation architecture and redistribution of insects moving on the plant surface, *Ecol. Model.* **155**, 149 (2002).
- [20] T. M. Elliott and J. F. Wheeler, Biased random walks on random combs, *J. Phys. A: Math. Theor.* **40**, 8265 (2007).
- [21] S. Havlin and D. ben Avraham, Diffusion in disordered media, *Adv. Phys.* **36**, 695 (1987).
- [22] D. Bertacchi, Asymptotic behavior of the simple random walk on the 2-dimensional comb, *Electron. J. Probab.* **11**, 1184 (2006).
- [23] B. Durhuus, T. Jonsson, and J. F. Wheeler, Random walks on combs, *J. Phys. A: Math. Gen.* **39**, 1009 (2006).
- [24] E. Agliari, A. Blumen, and D. Cassi, Slow encounters of particle pairs in branched structures, *Phys. Rev. E* **89**, 052147 (2014).
- [25] E. Agliari, F. Sartori, L. Cattivelli, and D. Cassi, Hitting and trapping times on branched structures, *Phys. Rev. E* **91**, 052132 (2015).
- [26] A. Rebenshtok and E. Barkai, Occupation times on a comb with ramified teeth, *Phys. Rev. E* **88**, 052126 (2013).
- [27] R. Burioni, D. Cassi, G. Giusiano, and S. Regina, Anomalous diffusion and hall effect on comb lattices, *Phys. Rev. E* **67**, 016116 (2003).
- [28] G. Forte, R. Burioni, F. Cecconi, and A. Vulpiani, Anomalous diffusion and response in branched systems: a simple analysis, *J. Phys. Condens. Matter* **25**, 465106 (2013).
- [29] N. Korabel and E. Barkai, Paradoxes of Subdiffusive Infiltration in Disordered Systems, *Phys. Rev. Lett.* **104**, 170603 (2010).
- [30] E. Baskin and A. Iomin, Superdiffusion on a Comb Structure, *Phys. Rev. Lett.* **93**, 120603 (2004).
- [31] A. Iomin and E. Baskin, Negative superdiffusion due to inhomogeneous convection, *Phys. Rev. E* **71**, 061101 (2005).
- [32] C. Van den Broeck, Waiting Times for Random Walks on Regular and Fractal Lattices, *Phys. Rev. Lett.* **62**, 1421 (1989).
- [33] D. Campos and V. Méndez, Reaction-diffusion wave fronts on comblike structures, *Phys. Rev. E* **71**, 051104 (2005).
- [34] D. Campos, J. Fort, and V. Méndez, Transport on fractal river networks: Application to migration fronts, *Theor. Pop. Biol.* **69**, 88 (2006).

- [35] B. Kahng and S. Redner, Scaling of the first-passage time and the survival probability on exact and quasi-exact self-similar structures, *J. Phys. A: Math. Gen.* **22**, 887 (1989).
- [36] V. Méndez, S. Fedotov, and W. Horsthemke, *Reaction-Transport Systems: Mesoscopic Foundations, Fronts, and Spatial Instabilities* (Springer, New York, 2010).
- [37] S. I. Denisov and W. Horsthemke, Anomalous diffusion of particles driven by correlated noise, *Phys. Rev. E* **62**, 7729 (2000).
- [38] D. Villamaina, A. Sarracino, G. Gradenigo, A. Puglisi, and A. Vulpiani, On anomalous diffusion and the out of equilibrium response function in one-dimensional models, *J. Stat. Mech.: Theor. Exp.* (2011) L01002.
- [39] I. Podlubny, *Fractional Differential Equations* (Academic, San Diego, 1999).
- [40] H. Bateman, *Higher Transcendental Functions* (McGraw-Hill, New York, 1953), Vol. I–III.